

Effects of compatilizers on the cellular structures, interfacial morphologies and mechanical properties of PP foam composites

Ji-Nian Yang, * Zi-Quan Li, * Jin-Song Liu

*College of Materials Science and Technology, Nanjing University of Aeronautics and Astronautics, Nanjing 210016, P. R. China; e-mail: yang_jinian@nuaa.edu.cn; ziquanli@nuaa.edu.cn

(Received: 26 April, 2010; published: 31 July, 2011)

Abstract: The short glass fiber (SGF)/polypropylene (PP) and ethylene-1-octene copolymer (POE)/SGF/PP foam composites were prepared by extrusion and subsequent post-foaming process in designed dies. The compatilizers, maleic anhydride grafted PP (PP-g-MAH) and maleic anhydride grafted POE (POE-g-MAH), were employed to improve the performance of the foam composites, respectively, and their influences on the cellular structures, interfacial morphologies and mechanical properties of PP foam composites were investigated. It was found that the compatilizers resulted in modified PP foam composites characterized by uniform cell size distribution, reduced cell size and increased cell density except POE/SGF/PP with POE-g-MAH. The obvious enhanced SGF-matrix interfacial bonding was observed from the SEM examination, and POE-q-MAH also facilitated the compatibility between elastomeric particles and matrix. Testing results indicated that, by the introduction of PP-g-MAH or POE-g-MAH, the mechanical properties of PP foam composites were significantly improved, and it seemed that the PP-g-MAH was more effective in strengthening the flexural and compressive strength while POE-g-MAH greatly increased the impact toughness.

Keywords: polypropylene; foam composites; compatilizer; mechanical property

Introduction

Polypropylene (PP) foam has obtained an extensive attention from researchers all over the world since it was developed in early 1970s. Compared with the traditional polystyrene (PS) and polyurethane (PU) foams, PP foam is more environmental-friendly possessed of outstanding biodegradability and retrievability. Nowadays, it has been widely applied in many industrial fields because of the high strength-to-weight ratio, excellent heat and sound insulations, good energy or mass absorption as well as chemical and water resistances [1-3]. However, the application of PP foam in engineering materials requesting high strength, stiffness and toughness would be somewhat limited due to the intrinsic shortcomings of polymeric foams and the relatively poor impact resistance of PP when subjected to impact load. It is still a challenge, therefore, to design and develop advanced PP foam with good performance and processibility for the wider application range.

According to literatures, the fabrication of foam composites by introducing short glass fibers (SGF) into the polymer matrix is a considerable method to enhance the tensile and compressive strength and to improve the thermal stability as well as cellular structure, as has been well confirmed by the phenolic [4-5], epoxy [6-7] and polyurethane [8-9] foams. Zhang [10] and Bledzki [11-12] et al. studied the influences

of wood fiber content on the microstructure and properties of PP foam composites, and it was reported that the extra-addition of 5 wt. % interfacial compatilizer could lead to an improvement up to 80% in the physico-mechanical properties.

For the sake of overcoming the low impact resistance of PP matrix, a soft elastomer is generally utilized and the most representative one is ethylene-1-octene copolymer (POE). The POE can lead to a significant increase in impact toughness of PP [13-16] and it is also expected to bring on a similar influence on the PP foam. In addition, Tjong et al [17] found that it was the co-incorporation of SGF and elastomer that could compensate the reduction in strength and stiffness resulted from elastomer [14-15] and maintain a stiff-toughness balance of the SGF/elastomer/PP hybrid composites.

Up to now, little information is available on PP foam composites reinforced by SGF or/and toughened by POE, let alone the application of interfacial compatilizer in PP foam composites. Therefore, the aims of the present work were to prepare the binary (SGF/PP) and ternary (POE/SGF/PP) foam composites with and without the interfacial compatilizers (maleic anhydride grafted PP, PP-g-MAH and maleic anhydride grafted POE, POE-g-MAH), and then to examine the cellular structures, interfacial morphologies and mechanical properties of PP foam composites.

Results and discussion

Cellular structures

Fig. 1 showed the SEM micrographs and corresponding bubble-size distribution of binary (SGF/PP) PP foam composites. As was clearly seen in Fig. 1, the cell numbers of SGF/PP1 and SGF/PP2 were increased compared with SGF/PP0 foam composites, though the cellular morphologies seemed hardly changed and still exhibited closed spherical-like bubbles in the presence of PP-g-MAH or POE-g-MAH. Therefore, both PP-g-MAH and POE-g-MAH improved the foaming effect of binary PP foam composites with a reduction of average cell diameter from 0.646 mm to 0.419 mm (and 0.420 mm) as well as a nearly four-fold increase in cell density (Tab. 1). Furthermore, the range of cell size distribution got narrow from 0.1-1.3 mm for SGF/PP0 to 0.15-0.85 mm for SGF/PP1, and to 0.15-0.95 mm for SGF/PP2, which, together with the obvious decreased variance of cell diameters (from 0.0783 to 0.0221), reveals that bubble-size distribution was more uniform. Possible reason could be that compatilizer plays a great role of strengthening the interfacial bonding between SGF and matrix, thus helping the dispersion of SGF in the polymer matrix. As a result, the melt strength will be improved which is attributed to the enhanced interactions amongst the SGF and polymers, thus facilitating the bubble stabilization without cell coalescence or rupture.

The better foaming effect of POE/SGF/PP0 could be seen from Fig. 2(a) in comparison with SGF/PP0, and it exhibited a nearly 30% reduction in average cell diameter and more than twofold increase in cell density as well as the variance declined to 0.0373 (Tab. 1). This indicated that the coexistence of POE and SGF, as well as their interaction, favored the formation of finer and more uniform bubbles than that of single SGF. However, the foaming effect changed when the compatilizers were introduced into the ternary PP composites, and the PP-g-MAH had a positive effect on the bubble size, distribution and cell density of POE/SGF/PP1 with well developed and uniform cellular structures (Fig. 2(b)), just as on SGF/PP1, whereas

POE/SGF/PP2 had relative larger and many un-regular cells compared with that of POE/SGF/PP0 and was rather different from SGF/PP2 (Fig. 2(c)).

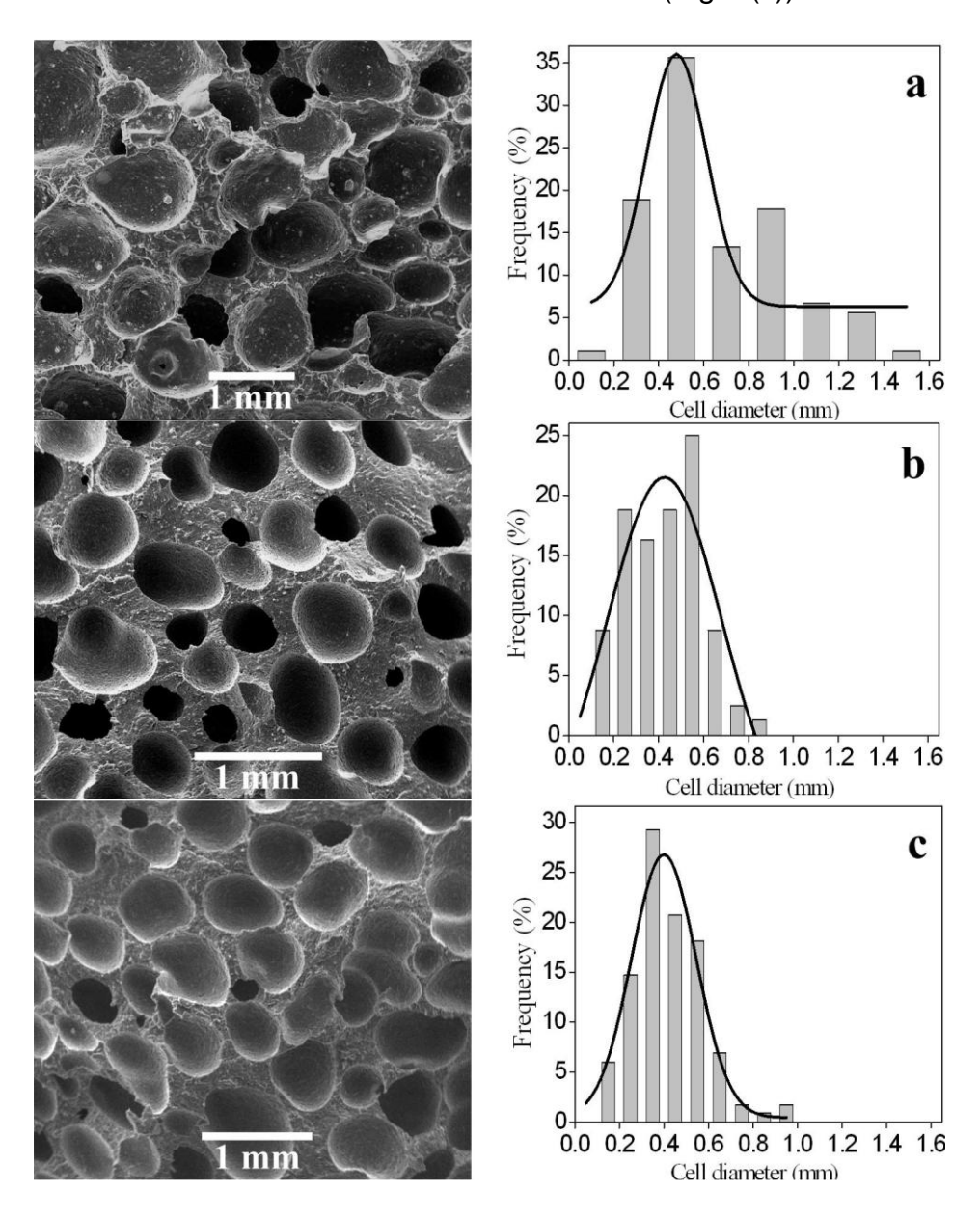


Fig. 1. SEM micrographs and bubble-size distribution (histogram) of binary PP foam composites: (a) SGF/PP0; (b) SGF/PP1; (c) SGF/PP2.

Tab. 1. Morphological parameters of SGF/PP and POE/SGF/PP foam composites.

Samples	Diameter (mm)	Cell density (cells·cm ⁻³)	Variance
SGF/PP0	0.646	3,581	0.0783
SGF/PP1	0.419	13,124	0.0229
SGF/PP2	0.420	13,031	0.0221
POE/SGF/PP0	0.470	8,692	0.0373
POE/SGF/PP1	0.450	9,903	0.0246
POE/SGF/PP2	0.610	3,976	0.0484

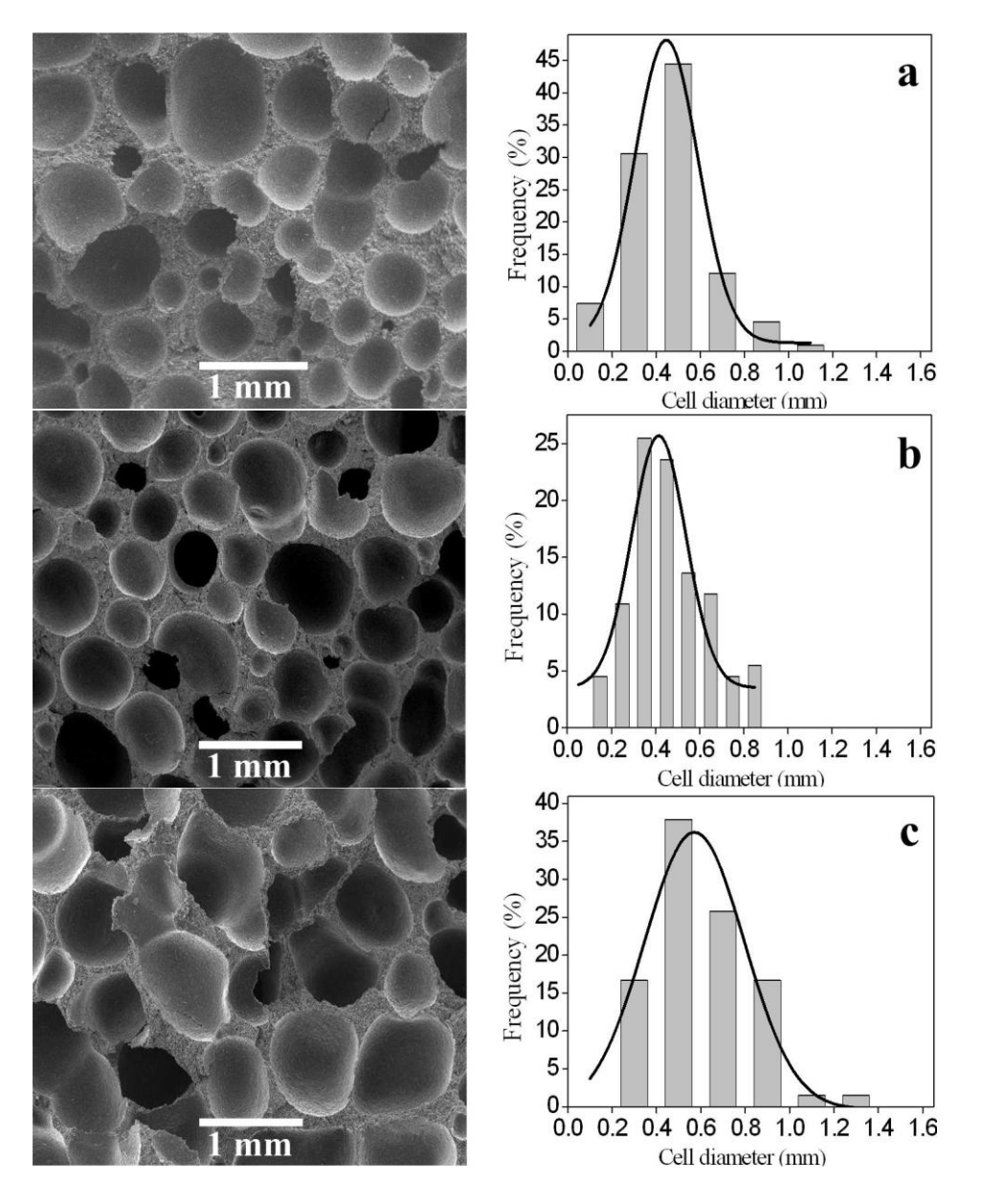


Fig. 2. SEM micrographs and bubble-size distribution (histogram) of ternary PP foam composites: (a) POE/SGF/PP0; (b) POE/SGF/PP1; (c) POE/SGF/PP2.

Morphologies

Fig. 3 presented the interfacial morphologies between SGF, elastomers and matrix in the impact fracture surfaces of PP foam composites. As was seen from the micrographs, the SGF was randomly distributed and the elastomeric phases (POE-g-MAH) acted as particles dispersing in the matrix and around the SGF. Fig. 3(a) showed that there were a few residual material parts left on the surface of reinforcing fibers in the foam composites (SGF/PP0) prepared with SGF treated by silane coupling agent, which indicated that failure occurred mainly at the fiber-matrix interface as a result of the relative poor interfacial adhesion between SGF and polymer matrix. In contrast, bulky matrix bonded firmly to the SGF surface, as well as the large contact area between the matrix and SGF of SGF/PP1 and SGF/PP2, suggested that failure increasingly occurred within matrix and the interfacial bonding between SGF and matrix was significantly improved with the existence of PP-g-MAH or POE-g-MAH (Fig.3(b) and 3(c)). It is thought that the MAH functional groups

generated from the compatilizers could polarize the non-polar matrix and promote the compatibility between the hydrophilic nature of SGF and the hydrophobic PP main phase. In addition, the ability of the MAH groups to react with —NH₂ groups on the SGF surface makes it possible to form the chemical combination instead of physic-mechanical adhesion, therefore facilitating further enhancement in the SGF-matrix interfacial performances. The chemical reaction may take place between compatilizers and the SGF as follows [18-19]:

$$\begin{array}{c} O \\ R - CH - C \\ CH_{2} - C \\ O + NH_{2} - (CH_{2})_{3} - Si \\ \hline \end{array}$$

$$\begin{array}{c} O \\ R - CH - C \\ CH_{2} - C \\ O \\ O \\ \end{array}$$

$$\begin{array}{c} O \\ N - (CH_{2})_{3} - Si \\ \hline \end{array}$$

$$\begin{array}{c} O \\ H_{2}O \\ \hline \end{array}$$

$$\begin{array}{c} O \\ N - (CH_{2})_{3} - Si \\ \hline \end{array}$$

$$\begin{array}{c} O \\ H_{2}O \\ \hline \end{array}$$

$$\begin{array}{c} O \\ D \\ \hline \end{array}$$

$$\begin{array}{c} O \\ D \\ D \\ \hline \end{array}$$

$$\begin{array}{c} O \\ D \\ D \\ \hline \end{array}$$

$$\begin{array}{c} O \\ D \\ D \\ \hline \end{array}$$

$$\begin{array}{c} O \\ D \\ D \\ \hline \end{array}$$

$$\begin{array}{c} O \\ D \\ D \\ \hline \end{array}$$

$$\begin{array}{c} O \\ D \\ D \\ D \\ \hline \end{array}$$

$$\begin{array}{c} O \\ D \\ D \\ D \\ \hline \end{array}$$

$$\begin{array}{c} O \\ D \\ D \\ D \\ \hline \end{array}$$

Fig. 3. SEM micrographs showing impact fracture surfaces of (a) SGF/PP0; (b) SGF/PP1; (c) SGF/PP2; (d) POE/SGF/PP0; (e) POE/SGF/PP1 and (f) POE/SGF/PP2.

It was interesting to note that the POE-g-MAH particles not only dispersed around the SGF but adhered firmly to the surfaces of drawn fibers (Fig. 3(c)). This novel configuration meant the possible interfacial interaction taking place between POE-g-MAH particles and SGF, which could be also attributed to the amidation reaction of anhydride groups with amino groups [18-19]. Moreover, the POE-g-MAH particles seemed not so spherical and no evident phase separation was observed in Fig. 3(c), i.e. the POE-g-MAH particles did not exhibit droplet-matrix morphologies as POE particles behaved in Fig. 3(d), revealing that the POE-g-MAH might be more compatible with the matrix than the POE.

The interfacial interactions developed in the ternary PP foam composites were more complex in comparison with that of binary PP foam composites (Fig. 3(d)~(f)). The similar improved interfacial bonding between SGF and the polymer matrix was observed as expected in POE/SGF/PP1 and POE/SGF/PP2 compared with POE/SGF/PP0 resulted from the introduction of compatilizers, as had been

discussed previously. The interfacial structures between POE particles and matrix seemed not to change in POE/SGF/PP1 modified with PP-g-MAH (Fig. 3(e)), showing the same typical droplet-matrix morphologies as that of exhibited in POE/SGF/PP0 (Fig. 3(d)), whereas the structures behaved differently POE/SGF/PP2 with the presence of POE-g-MAH (Fig. 3(f)). The elastomeric particles (POE and POE-g-MAH) were all embedded in PP matrix and almost no isolated bare elastomeric particles appeared on the fracture surface of composites. Compared with Fig. 3(d) and 3(e), the POE-g-MAH substantially improved the elastomeric particlematrix interfacial adhesion. The difference between the two compatilizers could mainly be explained by the higher affinity of POE-g-MAH with POE due to their same backbones than that of PP-q-MAH. Besides, the compatibility of POE-q-MAH with the matrix also offers partial contribution to this evolution of embedded morphologies. Nevertheless, the embedded structures of elastomeric particles in matrix may result in the sacrifice of interactions between POE particles and SGF simultaneously, which is likely to decrease the melt strength, thus it could be one of the reasons of the deterioration in foaming effect of POE/SGF/PP2, as shown in Fig. 2(c) and Tab. 1.

Mechanical properties

Fig. 4 illustrated the impact toughness of PP foam composites. Apparently, of all samples, SGF/PP0 exhibited the lowest impact toughness of 26.15kJ/m². By adding PP-g-MAH and POE-g-MAH into binary system, the impact toughness were heightened to 35.78kJ/m² for SGF/PP1 (36.8% improvement) and 46.23kJ/m² for SGF/PP2 (76.8% improvement), respectively.

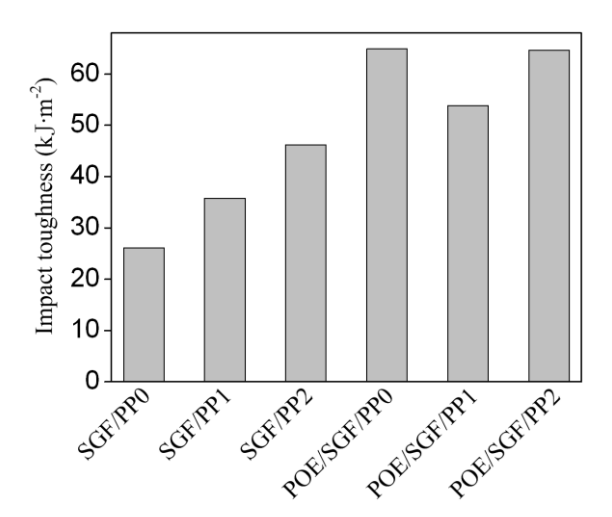


Fig. 4. Impact toughness of PP foam composites.

According to the nature of foams and principles of fiber reinforced composites, the cell deformation and fiber-matrix interfacial de-bonding are thought to be the two major mechanisms of energy absorption of the fiber reinforced foam composites when subjected to the impact testing [20-21]. On one hand, it is the fact of great improvements in the foaming effect characterized by fine and uniform cellular structures of SGF/PP1 and SGF/PP2 (Fig. 1(b) and (c)) that make them be much more effective than SGF/PP0 in consuming energy before materials crashed to pieces. On the other hand, the modified interfacial adhesion (Fig. 3(b) and (c)) also allows relative larger amounts of energy to be dissipated by way of enlarged areas of

interfacial de-bonding and prolonged paths of crack propagation during the process of fibers pulled out from matrix. As a result of that, the impact toughness increased understandably.

Moreover, it was also noticed that the impact toughness of SGF/PP2 was much higher than that of SGF/PP1, the increase rate of former was more than twice as high as the latter, which could be attributed to the unique morphologies (Fig (3)). The fact of POE-g-MAH particles adhered firmly to the surface of SGF and simultaneously inset into the PP matrix could give rise to an increased drawn resistance and prolonged crack propagating paths when SGF was drawn from the matrix, and thus much more impact energy could be consumed.

The maximum impact toughness exhibited in Fig. 4 was 64.89kJ/m² belonged to POE/SGF/PP0. In general, the impact toughness of the ternary system was much higher than that of the binary system. This tremendous increase in impact toughness of ternary PP foam composites is mainly due to the remarkable elastomer-toughening effect of POE (or/and POE-g-MAH) explained by the crazing/shear band interaction theory [22], which could be one of the reasons for much greater improvement of POE-g-MAH than PP-g-MAH in the impact toughness of binary system.

Moreover, Fig. 4 also revealed that either PP-g-MAH or POE-g-MAH mildly decreased the impact toughness of ternary system. The declined impact toughness for POE/SGF/PP1 could be resulted from the incorporation of brittle PP-g-MAH, which decreases the relative mass fraction of POE. This reduction of POE may counteract or even conceal the positive influence resulted from improved foaming effect and interfacial properties on the impact toughness, and therefore the impact toughness decreased. However, the reason for POE/SGF/PP2 would be the deterioration of cellular structures slightly weakening the energy absorption.

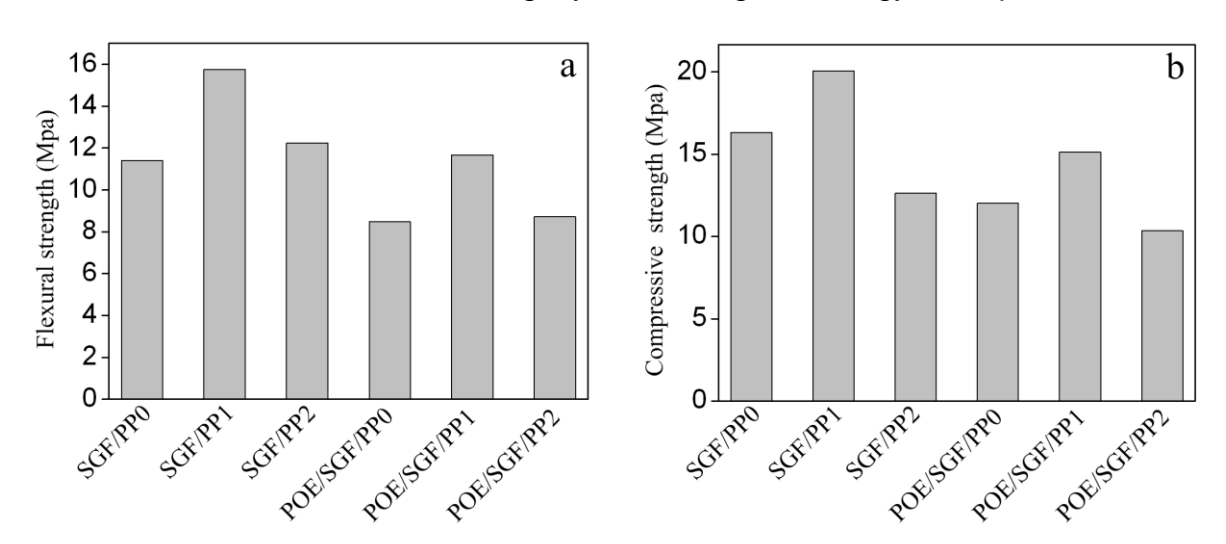


Fig. 5. Flexural and compressive strength of PP foam composites: (a) flexural strength, and (b) compressive strength.

The flexural and compressive properties were used to determine the strength of PP foam composites. As was seen from Fig. 5, with the addition of PP-g-MAH, the flexural and compressive strength of SGF/PP1 were increased from 11.41MPa and 16.31MPa to 15.76MPa (38.1% improvement) and 20.06MPa (23.0% improvement), respectively. In contrast, only a slight improvement (7.3%) on flexural strength of

SGF/PP2 was obtained, while the compressive strength decreased by incorporation of POE-g-MAH. The flexural and compressive strength of POE/SGF/PP0 decreased in comparison with SGF/PP0, which would be mainly attributed to the existence of POE characterized by low strength. Similarly, adding PP-g-MAH into ternary system led to an improvement in both flexural and compressive strength of POE/SGF/PP1, while POE-g-MAH seemed to have little or even worse influence on the strength of POE/SGF/PP2; i.e. the binary and ternary PP foam composites exhibited the similar variation tendency in strength when using PP-g-MAH or POE-g-MAH as the compatilizer.

From above SEM observations, the most contribution of the compatilizers to the binary or ternary PP foam composites is generally believed to be their significantly enhancing the interfacial adhesion between SGF and the matrix (Fig. 3). Then the applied stress can be more efficiently transferred through the interfaces and borne by the higher strength fibers, thus the mechanical properties of PP foam composites should be strengthened. According to Fig. 5, the PP-g-MAH led to the increase in flexural and compressive strength of SGF/PP1 and POE/SGF/PP1 indeed. However, POE-g-MAH behaved much lower strength than PP-g-MAH and the matrix, showing an inevitable trend of making POE-g-MAH less competitive than PP-g-MAH in increasing the strength of PP foam composites. Consequently, the improvement in flexural strength of SGF/PP2 and POE/SGF/PP2 was limited, while the compressive strength decreased in the presence of POE-g-MAH.

Conclusions

In this study, the cellular structures, interfacial morphologies and mechanical properties of the binary (SGF/PP) and ternary (POE/SGF/PP) foam composites modified with compatilizers were investigated. The incorporation of PP-g-MAH and POE-g-MAH led to remarkable improvement in foaming effect, with a more uniform cell size distribution and up to 35% reduction in average cell diameters as well as nearly fourfold increase in cell density of the modified PP foam composites except POE/SGF/PP2.

SEM observation demonstrated that the interfacial adhesion between SGF and the PP matrix was enhanced remarkably in presence of compatilizers, while POE-g-MAH also promoted the compatibility of elastomeric particles and matrix, exhibiting a particle-embedded configuration instead of the typical droplet-matrix morphology in ternary system.

The mechanical tests revealed that the nature of compatilizers largely determined the toughness or strength of PP foam composites, i.e. the PP-g-MAH was more favourable for strengthening the flexural and compressive strength, while the POE-g-MAH seemed to benefit increasing the impact toughness of PP foam composites.

Experimental part

Materials

Commercial grade isotactic polypropylene (PP, PPH-XD-140) was kindly supplied by Nanjing Jinling Plastic & Petrochemical Co., Ltd (China). Low density polyethylene (LDPE, 6634F) was provided by Formosa Plastics Corporation (Taiwan). The elastomer used was ethylene-1-octene copolymer (POE, Engage 8180) purchased from DuPont Dow Chemical Company (USA). The two compatilizers used were

maleic anhydride grafted PP (PP-g-MAH, HD900P) and maleic anhydride grafted POE (POE-g-MAH, HD800E). Both are products of Nanjing Huadu Technology Co., Ltd (China). The short glass fiber (SGF) pretreated with silane coupling agent (A1100) was provided by Nanjing Fiberglass R&D Institude (China) with diameter of $8\sim15\mu m$ and aspect ratio of $5\sim10$, acting as a reinforcement material. Compounded foaming agent consisted of azodicarbonamide (95% purity, supplied by Jiangsu Sopo group, China) and ZnO and SiO₂ (acted as accelerant and nucleator, respectively and both commercial available) was pre-mixed homogeneously with a mass ratio of 1:0.1:0.15.

Sample preparation

According to our previous work [23], LDPE was employed as a co-blend modifier and PP/LDPE (80/20, mass ratio) was adopted as base resin. The foam composites were prepared according to the formulae shown in Tab. 2. Firstly, all materials were dried separately in ovens for 24 h at 60°C before premixing in a SHR-10A high speed mixer, and then the mixtures were fed into a CM-30 single-screw extruder. The temperature profiles of the extruder were set at 160, 175, 180, 175, and 170 °C from feeding zone to die. The compounded extrudates were immediately quenched in water and cooled in air to ambient temperature and subsequently chopped into granules. Finally, the prepared granules dried at 100°C for 24 h were packed into a designed dies and heated in a oven at 170~175°C for 2~2.5h to form final PP foam composites. The densities of samples were controlled at 0.47~0.48 g·cm⁻³.

Tab. 2. Formulae of PP foam composites (phr).*

Samples	PP	LDPE	SGF	POE	PP-g-MAH	POE-g-MAH
SGF/PP0	80	20	20	_	_	_
SGF/PP1	80	20	20	_	8	_
SGF/PP2	80	20	20	_	_	8
POE/SGF/PP0	80	20	20	20	_	_
POE/SGF/PP1	80	20	20	20	8	_
POE/SGF/PP2	80	20	20	20	_	8

^{*}All composites contained 12 phr of compounded foaming agent.

Performance characterization

Impact, bending and compression tests were carried out at room temperature to evaluate the mechanical performances of PP foam composites. The un-notched Charpy impact test was performed by using a XJ-300A impact tester with a sample dimension of $75 \times 15 \times 15 \text{ mm}^3$ and impact toughness calculated by dividing the impact work by the cross-sectional area of the sample. The three-point bending test and quasi-static compression test, with sample sizes of $75 \times 15 \times 15 \text{ mm}^3$ and $50 \times 50 \times 30 \text{ mm}^3$, respectively, were both done in a computer-controlled CMI 5150 universal testing machine operated with a crosshead speed of 2 mm/min. The tests were stopped when material failed for bending and 50% deflection relative to the initial thickness reached for compression. Both flexural and compressive strength were obtained as outputs from the computer. All results were the average of at least five measurements for each type.

The impact fractured surfaces of PP foam composites were selected and coated with a thin layer of gold before their examination in a scanning electron microscope (SEM,

QUTAN 200 and JSM-5610LV) for the observation of cellular structures, distribution of SGF and elastomer particles in the matrix as well as the interfacial adhesion between SGF, elastomer and matrix. Approximate 50~100 cells from the micrographs were then analyzed using Image-Pro Plus Software to obtain the average cell diameter, bubble-size distribution and variance of cell size, which, together with the cell density calculated according to the reference [24], were used to determine the foaming effect of PP foam composites.

Acknowledgements

The authors gratefully acknowledge the financial support of Natural Science Foundation of Jiangsu Province of China (BK2009379) and also thank Xiangyin Mo, Keyu Wang, Xiaoyun Hu, Lei Wang, and Qin Wang for their assistance in generating the experimental data.

References

- [1] He, J.M. Eng Plast Appl. 2002, 30, 54. (in Chinese with English abstract)
- [2] Jahani, Y.; Barikani, M. Iran Polym J. 2005, 14, 361.
- [3] Han, D.H.; Jang, J.H.; Kim, H.Y.; Kim, B.N.; Shin, B.Y. *Polym Eng Sci.* **2006**, 46, 431.
- [4] Shen, H.B.; Nutt, S. Compos Part A-Appl S. 2003, 34, 899.
- [5] Desai, A.; Auad, M.L.; Shen, H.B.; Nutt, S. J Cell Plast. 2008, 44, 15.
- [6] Karthikeyan, C.S.; Sankaran, S.; Kishore, A. Mater Lett. 2004, 58, 995.
- [7] Alonso, M.V.; Auad, M.L.; Nutt, S. Compos Part A-Appl S. 2006, 37, 1952.
- [8] Yang, Z.G.; Zhao, B; Qin, S.L.; Hu, Z.F.; Jin, Z.K.; Wang, J.H. *J Appl Polym Sci.* **2004**, 92, 1493.
- [9] Mkrtchvan, L.; Maier, M. *Plast Rubber Compos.* **2007**, 36, 445.
- [10] Zhang, S.W.; Rodrigue, D.; Riedl, B. *Polym Compos.* **2005**, 26, 731.
- [11] Bledzki, A.K.; Faruk, O. Cell Polym. 2002, 21, 417.
- [12] Bledzki, A.K.; Faruk, O. J Cell Plast. 2006, 42, 77.
- [13] Da Silva, A.L.N.; Rocha, M.C.G.; Coutinho, F.M.B.; Bretas R.E.S.; Farah M. *Polym Test.* **2002**, 21, 647.
- [14] Paul, S.; Kale, D.D. J Appl Polym Sci. 2000, 76, 1480.
- [15] McNally, T.; McShane, P.; Nally, G.M.; Murphy, W.R.; Cook, M.; Miller, A. *Polym.* **2002**, 43, 3785.
- [16] Yang, J.H.; Zhang, Y.; Zhang, Y.X. *Polym.* **2003**, 44, 5047.
- [17] Tjong, S.C.; Xu, S.A.; Li, R.K.Y.; Mai, Y.W. J Appl Polym Sci. 2002, 86, 1303.
- [18] Bikiaris, D.; Matzinos, P.; Larena, A.; Flaris, V.; Panayiotou, C. *J Appl Polym Sci.* **2001**, 81, 701.
- [19] Zheng, A.; Wang, H.G.; Zhu, X.X.; Masuda, S. Compos Interface. **2002**, 9, 319.
- [20] Gibson, L.J.; Ashby, M.F. *Cellular Solids: structure and properties,* Cambridge University Press: Cambridge, **1997**.
- [21] Tjong, S.C.; Xu, S.A.; Li, R.K.Y.; Mai Y.W. Polym Int. 2002, 51, 1248.
- [22] Jang, B.Z.; Uhlmann, D.R.; Vander Sande, J.B. *J Appl Polym Sci.* **1985**, 30, 2485.
- [23] Li, Z.Q.; Ouyang, M.; Yang, J.N.; Zhou, H.Z. *J Nanjing Univ Aeronaut Astronaut.* **2006**, 38, 378. (in Chinese with English abstract)
- [24] Okamoto, M.; Nam, P.H.; Maiti, P.; Kotaka, T.; Nakayama, T.; Takada, M.; Ohshima, M.; Usuki, A.; Hasegama, N.; Okamoto, H. *Nano Lett.* **2001**, 1, 503.